ELSEVIER

Biochimica et Biophysica Acta 1467 (2000) 326–337

BIOCHIMICA ET BIOPHYSICA ACTA
BBA

www.elsevier.com/locate/bba

Conformational studies of sphingolipids by NMR spectroscopy. II. Sphingomyelin

C. Mark Talbott [a], Igor Vorobyov [a], Douglas Borchman [b], K. Grant Taylor [a], Donald B. DuPré [a], M. Cecilia Yappert [a,b,*]

[a] *Department of Chemistry, University of Louisville, Louisville, KY 40292, USA*
[b] *Department of Ophthalmology and Visual Sciences, University of Louisville, Louisville, KY 40292, USA*

Received 5 March 1999; received in revised form 18 April 2000; accepted 20 April 2000

Abstract

Sphingomyelin (SM) is the most prevalent sphingolipid in the majority of mammalian membranes. Proton and ^{31}P nuclear magnetic resonance spectral data were acquired to establish the nature of intra- and intermolecular H-bonds in the monomeric and aggregated forms of SM and to assess possible differences between this lipid and dihydrosphingomyelin (DHSM), which lacks the double bond between carbons 4 and 5 of the sphingoid base. The spectral trends suggest the formation of an intramolecular H-bond between the OH group of the sphingosine moiety and the phosphate ester oxygen of the head group. The narrower linewidth and the downfield shift of the resonance corresponding to **OH** proton in SM suggest that this H-bond is stronger in SM than in DHSM. The NH group appears to be involved predominantly in intramolecular H-bonding in the monomer. As the concentration of SM increases and the molecules come in closer proximity, these intramolecular bonds are partially disrupted and the NH group becomes involved in lipid–water interactions. The difference between the SM and DHSM appears to be not in the nature of these interactions but rather in the degree to which these intermolecular interactions prevail. As SM molecules cannot come as close together as DHSM molecules can, both the NH and OH moieties remain, on average, more intramolecularly bonded as compared to DHSM. © 2000 Elsevier Science B.V. All rights reserved.

Keywords: Sphingomyelin; Sphingolipid; H-bonding; Nuclear magnetic resonance; Conformation; Lipid–lipid interaction

1. Introduction

Sphingophospholipids or sphingomyelins (SMs) constitute the most common sphingolipids in mammalian membranes [1,2]. The enigmatic, sphinx-like nature of these molecules inspired their name over 100 years ago, when Thudicum [3] first recognized their presence in brain tissue. These molecules result from the addition of a polar head group, phosphorylcholine in most cases, to ceramides. SM is the most abundant sphingophospholipid and its structure, *N*-acyl-sphingosine-1-phosphorylcholine or ceramide-1-phosphorylcholine, was reported in 1927 [4]. The enantiomeric configuration in SMs of biological origin is D-*erythro*, in which OH and NH_2 groups attached to carbons 2 and 3, respectively, are in the 2*S*,3*R* configuration [5]. Tissues in which SM is the predominant phospholipid include the sheath of nerve cell axons, myelin (25%), erythrocytes (18%) [1,6] and ocular lenses from most mammalian species

* Corresponding author. Fax: +1-502-852-8149; E-mail: mcyappert@louisville.edu

0005-2736/00/$ – see front matter © 2000 Elsevier Science B.V. All rights reserved.
PII: S0005-2736(00)00229-7

(from 30% in rabbits to 70% in nuclear lens membranes of elephants) [7–10]. In human lenses, however, SM accounts for only 10 to 15% of the phospholipid content [11–13]. Interestingly and puzzlingly, human lens membranes contain high levels of dihydrosphingomyelin (DHSM) [13,14] in which the double bond between carbons 4 and 5 is not present.

As the flexibility of SM precludes the formation of high-quality crystals, the X-ray structure of SM has not been published. However, pioneering insight on the molecular arrangement of the ceramide portion of sphingolipids has been deduced from the crystal structures of several phospholipid constituents [15–17]. In the molecular arrangements proposed by Pascher [15] the orientation of the H-bond donors and acceptors of the amide group and the hydroxyl group could allow for lateral interactions with other lipid molecules. Bruzik, [18] on the other hand, proposed a conformational arrangement in which the hydroxyl group on carbon 3 of sphingosine is intramolecularly hydrogen-bonded to an ester oxygen of the phosphate group. Using X-ray diffractometry, Khare and Worthington [19] found that the diffraction spacings did not change in oriented SM bilayers exposed to different levels of humidity. Their results and those of Hui et al. [20] also indicated that the phosphorylcholine head group of SM lies parallel to the membrane forming a right angle with respect to the hydrocarbon chains. The thermotropic behavior of SM has been summarized by Barenholz and Thompson [21,22]. Their studies and those of Shipley et al. [23–25] as well as Bruzik and Tsai [26] indicate that the gel to liquid crystalline phase transition temperature and the enthalpy of the transition are related to the degree of hydration and the composition of the acyl chains.

Understanding the nature of inter- and intramolecular forces that establish the biomembrane architecture is of paramount importance [15–17,27] in the determination of the structural roles of two major sphingolipids in ocular lens membranes, SM and DHSM. With an average of 3 mol cholesterol per mol phospholipid [28,29], human lens membranes possess the highest levels of cholesterol found in all mammalian membranes. This fact and recent reports of the presence of buoyant clusters rich in SM and cholesterol in some cells [30–32], suggest that sphingolipids, in addition to the common bilayer arrangement, may also be present in non-bilayer structural domains within biomembranes. The conformations adopted by SM in these environments are unknown. To establish the possible nature of these conformers and the impact of bound water molecules on these arrangements, high-resolution nuclear magnetic resonance (NMR) spectroscopy has been applied to samples of SM in a variety of concentrations and hydration levels using chloroform as solvent. Because of the low dielectric constant of this solvent, SM goes from a monomeric form at very low concentrations to a reverse micellar arrangement at higher concentrations. In addition, due to enhanced van der Waals interactions as the hydrophobic tails of neighboring reverse micelles come into close proximity, the aggregated samples go from a fluid to a gel phase as the temperature is decreased. The results presented herein address the participation of the head group and interfacial region in intra- and intermolecular H-bonds for the different levels of aggregation and hydration. In addition, the observed trends are compared to those reported for DHSM, which lacks the double bond between carbons 4 and 5 [33].

2. Materials and methods

2.1. Sample preparation

SM, 99% from bovine brain, deuterated chloroform, $CDCl_3$, and deuterium oxide, D_2O, were obtained from Sigma (St. Louis, MO, USA) and used without further purification. Samples of SM ranging in concentration from 1.0 to 182 mM were prepared in $CDCl_3$. For all samples, the proper weight of SM, assuming an average molecular weight of 780 g/mol, was placed into each sample vial and $CDCl_3$ was added. The vial was then vortexed and heated for 10 s in a 50°C water bath until the sample dissolved and the solution turned clear. The sample was vortexed again. Samples prepared in this way contained bound water and are thus termed *partially hydrated*. The amount of water present in these samples was evaluated by integration of the ^1H resonance corresponding to the bound water molecules. The average of the integration indicated the presence of 2.5 ± 1 water molecules per SM for sample concentrations

above 10 mM. To study the effects of bound water, an analogous series of dehydrated samples was prepared. The dehydration process consisted of dissolving the appropriate amount of SM in $CDCl_3$ and then evaporating to dryness on a rotatory evaporator. The sample vial was then subjected to a vacuum level of 0.02 Torr for 24 h. Argon was used to void the vacuum and $CDCl_3$ was immediately added to the vial, followed by vortexing and heating steps described as for the partially hydrated samples. In most cases, no water resonance was detected. In some samples, however, a residual weak peak that integrated to less than half of a water molecule was observed. These samples are referred to as *dehydrated samples. Fully hydrated samples* were prepared by adding 24 μl aliquots of D_2O to the partially hydrated samples. This ensured a water to lipid molar ratio in excess of 50.

2.2. NMR spectroscopic studies

One-dimensional proton spectra were obtained on a Bruker AMX 500 spectrometer. For ^1H spectra, a central frequency of 500.138 MHz was used with a sweep width of 15.15 ppm and a 32K data file. A central frequency of 202.46 MHz was used for ^{31}P NMR spectral acquisition, along with a sweep width of 5.01 ppm and a 16K data point. A proton decoupling frequency of 500.14 MHz was employed. For the variable temperature studies, the temperature ranged from 15 to 52°C. Spectra were processed with a line broadening of 1 Hz and phased using the Bruker AMX500 UXNMR (Bruker Instruments, Billerica, MA, USA). Further spectral evaluation and comparison was accomplished with GRAMS386 software (Galactic Industries, Salem, NH, USA).

3. Results

Fig. 1 shows the components and the labeling scheme for the SM molecule. This labeling is based on that used by Pascher for ceramide [15] and, as indicated in the accompanying report [33], includes the numbering of the choline head group as doubly primed labels. Previous studies have reported the assignment of ^1H NMR resonances [18,34]. The following results focus on the changes in ^1H and ^{31}P resonances as a function of temperature and concentration in $CDCl_3$. In addition, the importance of water in the average conformation of the molecule is indicated by the spectral differences observed between partially hydrated samples, which contained an average of 2.5 bound water molecules per phospholipid, and dehydrated samples, with less than half of a bound water molecule per SM. Given the relatively long time scale of the NMR experiment, the spectral trends reported in this section are representative of average conformational preferences of the sample at different levels of aggregation and hydration.

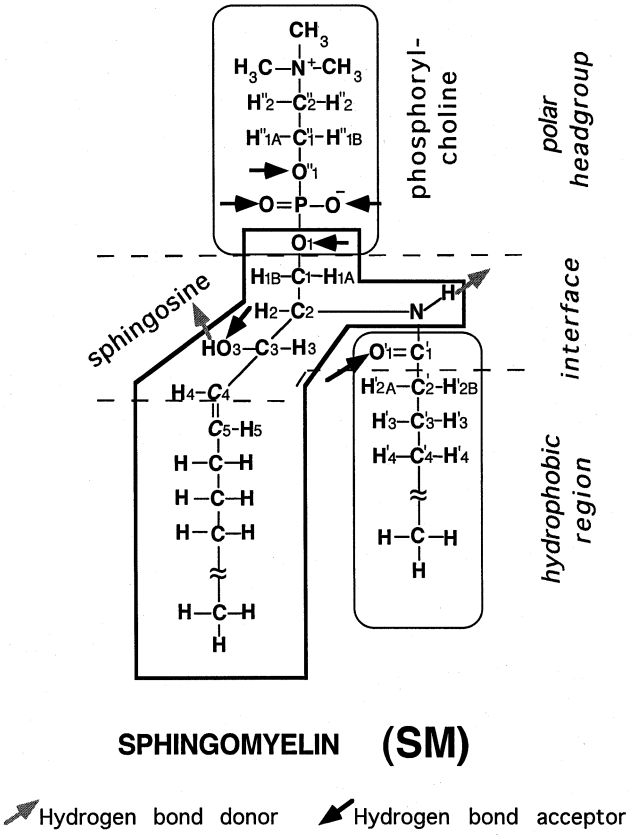

Fig. 1. Components, regions and atom numbering of SM.

3.1. Concentration- and temperature-dependent conformational studies

Concentrations of partially hydrated SM in $CDCl_3$ ranging from 1.0 to 182 mM were investigated by ^1H and ^{31}P NMR spectroscopy. In addition, each con-

centration was also studied at temperatures ranging from 15 to 52°C. The average ± S.D. of the chemical shifts measured in three independent runs for a given concentration are plotted as a function of concentration. A logarithmic scale was used for the abscissa to emphasize the changes that occur at the lower concentrations where SM molecules begin to form reverse micelles. The relative standard deviations (R.S.D.s) of most ^{1}H resonances were less than 0.6%, with the exception of the N**H** and O**H** resonances, which reached a maximal R.S.D. of 0.9%. The smooth curves shown in these plots are included to facilitate the observation of the trends reported here.

3.1.1. Head group region

Significant changes were observed in the resonances for all of the head group protons: **H**″1A, **H**″1B, **H**″2 and the tri-methyl protons $N^{+}(CH_3)_3$. Diastereotopic protons **H**″1A and B exhibited non-equivalent chemical shifts at the lower concentrations but appeared to be magnetically equivalent at the higher concentrations, as shown in Fig. 2. Protons **H**″2 exhibited a single resonance at all concentrations and temperatures investigated (not shown).

Fig. 3 shows the concentration dependence of the ^{31}P NMR chemical shift for the partially hydrated (solid symbols and lines) and dehydrated (open symbols and lines) samples at 32°C. With increasing temperatures, from 15 to 52°C, a downfield shift of (0.22 ± 0.08) ppm was seen in this resonance for concentrations above 10 mM (not shown). However, the overall change was more pronounced for the concentrations below 10 mM for which a downfield shift of (0.64 ± 0.07) ppm was observed as the temperature increased from 25 to 52°C.

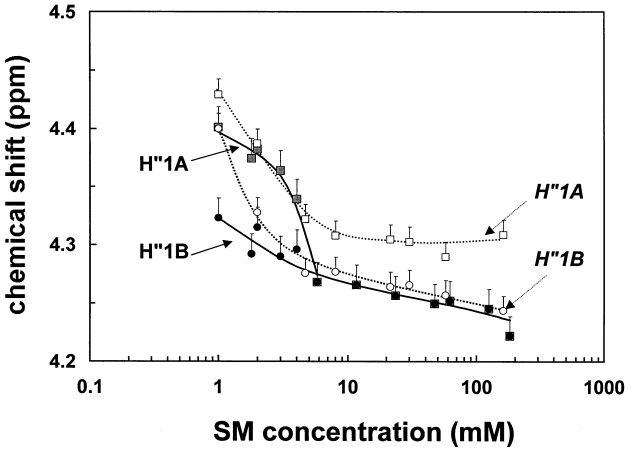

Fig. 2. Concentration dependence of the resonances corresponding to protons **H**″1A and B of the choline moiety at 32°C. Solid symbols and lines correspond to partially hydrated samples in $CDCl_3$. Open symbols and broken lines correspond to dehydrated samples in $CDCl_3$.

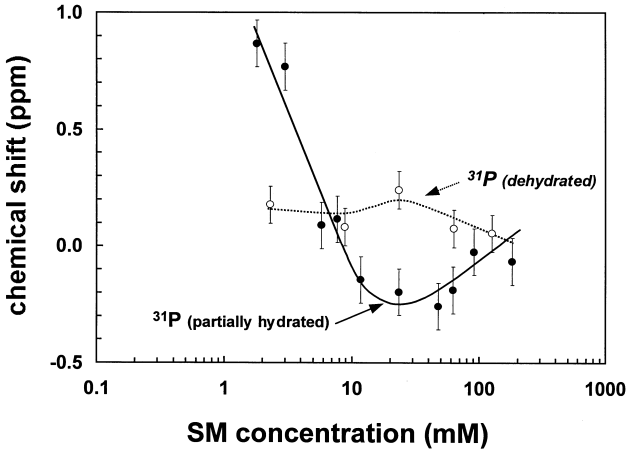

Fig. 3. Concentration dependence of the ^{31}P resonance corresponding to the phosphate head group at 32°C. Solid symbols and lines correspond to the partially hydrated samples in $CDCl_3$. Open circles and broken lines correspond to the dehydrated samples in $CDCl_3$.

3.1.2. Interfacial region

Several resonances corresponding to protons **H**1A, **H**1B, **H**2 and **H**3 were seen between 4.4 and 3.9 ppm. In addition, the proton resonance associated with the hydroxyl group (O**H**) attached to carbon C3 and the resonances corresponding to **H**4 and **H**5 across the double bond of sphingosine were in the spectral region between 5.0 and 6.0 ppm. The amide proton resonance, N**H**, exhibited a highly temperature- and concentration-dependent chemical shift which varied between 6.3 and 7.2 ppm.

Fig. 4 shows the concentration dependence of the resonances corresponding to geminal protons **H**1A and B and proton **H**3 for the partially hydrated and dehydrated samples. For partially hydrated samples (solid symbols and lines) **H**1A and B remained separated by (0.17 ± 0.03) ppm for concentrations above 10 mM. Below this concentration, the separation was enhanced. The **H**1A and B resonances for the dehydrated samples (open symbols and dotted

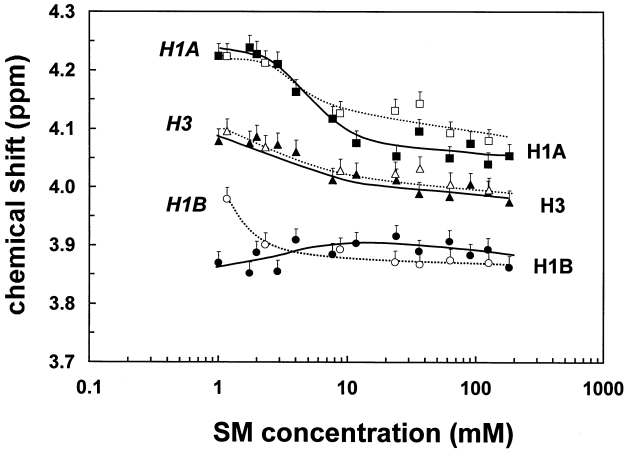

Fig. 4. Concentration dependence of the resonances corresponding to protons **H**1A and B, and **H**3 of the interfacial region at 32°C. Solid symbols and lines correspond to partially hydrated samples in $CDCl_3$. Open symbols and broken lines correspond to dehydrated samples in $CDCl_3$.

lines) with concentrations above 10 mM exhibited a difference of (0.24 ± 0.03) ppm in chemical shift, slightly higher than that seen in the partially hydrated samples. Below 10 mM, however, and unlike the partially hydrated samples, the two resonances shifted downfield. No significant changes were seen with concentration and hydration level in the **H**2 resonance (not shown).

Of the resonances for the interface protons, those corresponding to **H**1A and **H**3 were the most affected by temperature (data not shown). Increasing the temperature caused both resonances to move downfield. Over the temperature range investigated (15 to 52°C), the chemical shift increased by (0.08 ± 0.02) ppm for both resonances at lower concentrations, between 2 and 10 mM. At concentrations higher than 10 mM, the changes were less pronounced and measured to be (0.03 ± 0.01) and (0.05 ± 0.01) ppm for **H**1A and **H**3, respectively.

The changes observed in the N**H** resonance are plotted as a function of concentration at 32°C in Fig. 5 for the partially hydrated samples (solid symbols and lines) and dehydrated samples (open symbols and lines). For all concentrations of partially hydrated samples, the chemical shifts δ decreased as the temperature T increased. The temperature coefficient, $\Delta\delta/\Delta T$, was $-(0.011 \pm 0.001)$ ppm/°C for concentrations above 5 mM. Below 5 mM, the rate of change diminished to $-(0.006 \pm 0.002)$ ppm/°C. This low rate of change was also seen in the dehydrated samples.

Fig. 6 shows the concentration and temperature dependence of the O**H** resonance. The solid symbols in Fig. 6 represent the changes seen in the partially hydrated samples at 15°C. The chemical shift of this

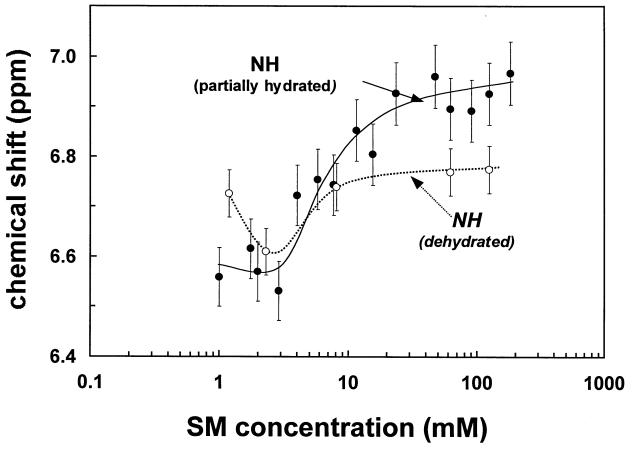

Fig. 5. Concentration dependence of the resonance corresponding to N**H** proton of the interface at 32°C. Solid symbols and lines correspond to partially hydrated samples in $CDCl_3$. Open symbols and broken lines correspond to dehydrated samples in $CDCl_3$.

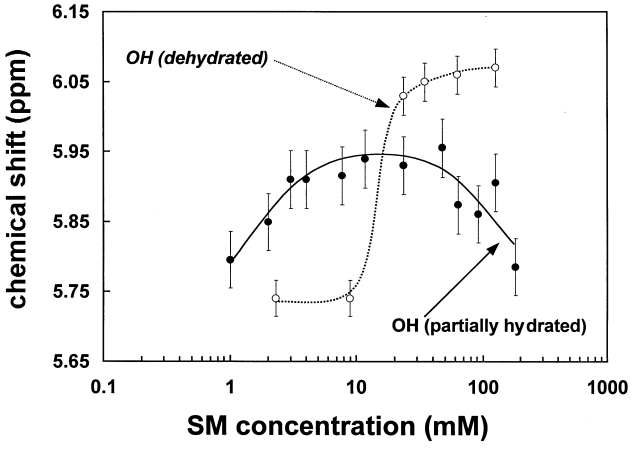

Fig. 6. Concentration dependence of the resonance corresponding to O**H** proton of the interfacial region of partially hydrated samples in $CDCl_3$. Solid symbols and lines correspond to partially hydrated samples in $CDCl_3$ at 15°C. Open symbols and broken lines correspond to dehydrated samples in $CDCl_3$ at 15°C.

resonance could be measured with greater precision at this low temperature. The faster rate of exchange at higher temperatures resulted in the broadening of the OH band. There was an upfield shift in the δ of this OH resonance as the temperature was increased. However, unlike the amide proton NH resonance, no changes in the value of $\Delta\delta/\Delta T$ were seen at the different concentrations. $\Delta\delta/\Delta T$ remained at $-(0.012 \pm 0.002)$ ppm/°C for all concentrations, regardless of the level of hydration.

3.1.3. Bound water

The level of hydration in the partially hydrated samples averaged (2.5 ± 1) water molecules per lipid molecule for sample concentrations above 10 mM. At lower concentrations, the integration of the water resonance reached up to 10 water molecules per lipid. These estimations were based on the integration of the H_2O resonance. The dependence of the chemical shift for this resonance with the concentration of SM (in logarithmic scale) is shown in Fig. 7 for two temperatures, 32 and 45°C. Three regions can be observed in the graph: (a) corresponding to the most diluted samples in which the chemical shift of water resonance was comparable to that of water impurities in the chloroform solvent, (b) which showed a fairly rapid increase in chemical shift with concentration as the concentration changed from about 3 mM to about 50 mM and (c) for which the change in chemical shift was reduced. The slopes for (b) and (c) represent the change in chemical shift (in ppm) per unit change in the logarithm of the concentration of SM (in mM) and were evaluated to be 1.86 ± 0.04 and 0.17 ± 0.08, respectively.

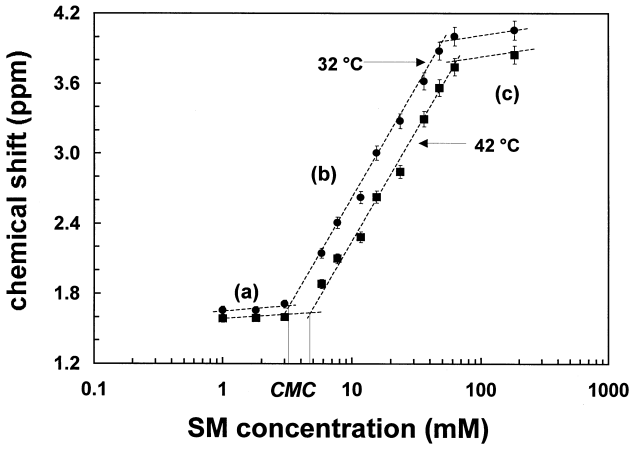

Fig. 7. Concentration dependence of the resonance corresponding to H_2O protons of water molecules bound to SM in $CDCl_3$. Regions (a), (b) and (c) are discussed in the text. The intercept of lines (a) and (b) is interpreted as the CMC.

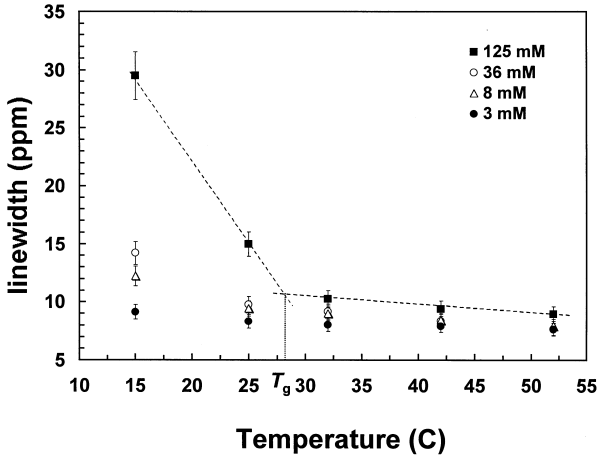

Fig. 8. Temperature dependence of the linewidth of the CH_2 resonance of the hydrophobic chains at different concentrations.

3.1.4. Hydrophobic region

The change with temperature in the linewidth of the CH_2 resonance corresponding to the hydrophobic chains is illustrated in Fig. 8 for several concentrations. For the highest concentration shown (125 mM), a significant change in linewidth was observed at (27 ± 1)°C. At the lower concentration shown (3 mM), no broadening was observed even at 15°C, the lowest temperature investigated.

3.2. Effect of hydration

The effect of the addition of 24 μl of D_2O to a partially hydrated 30 mM sample of SM in $CDCl_3$ is illustrated in Fig. 9. The ratio of water molecules per phospholipid exceeded 50. The resonances associated with the choline protons H″1, H″2 and $N^+(CH_3)_3$ (not shown) shifted upfield. The resonances for interface protons H1A and B exhibited opposite changes: H1A moved upfield and H1B downfield. As a result, the two resonances overlapped with each other and with the H3 resonance. Both the H2 and H3 resonances shifted upfield by 0.03 and 0.05 ppm, respectively.

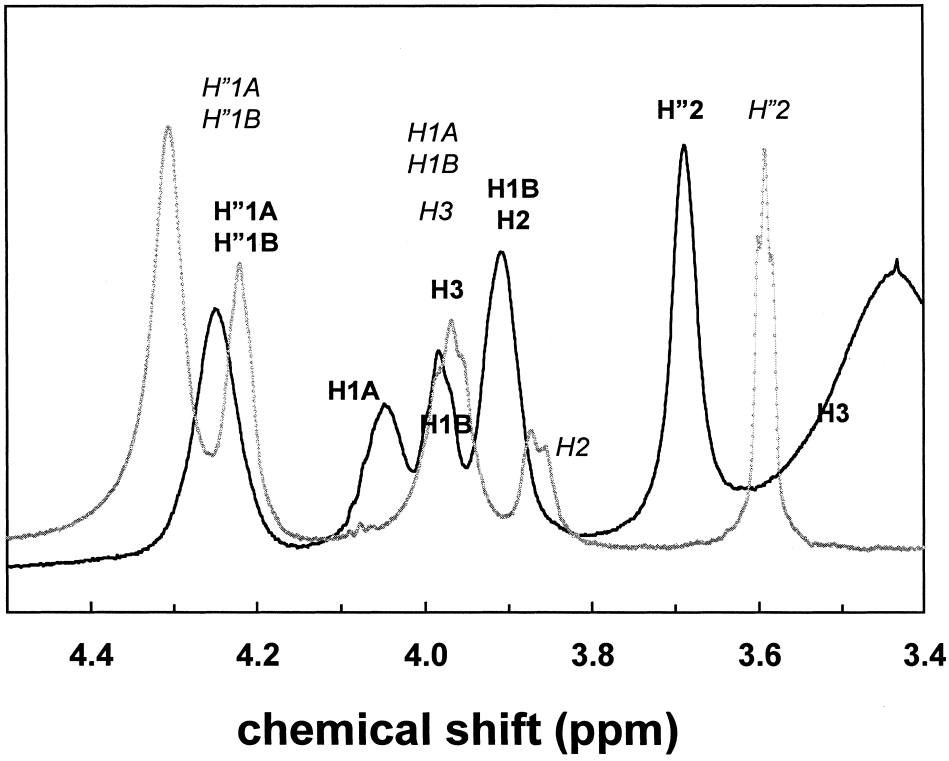

Fig. 9. Effect of D_2O addition to a 30 mM partially hydrated SM sample in $CDCl_3$. Solid lines represent the partially hydrated samples in $CDCl_3$. Lighter gray lines show the spectral traces obtained after addition of D_2O.

4. Discussion

4.1. Monomer to reverse micelle transition

The changes in spectral features observed for SM as a function of concentration in $CDCl_3$ result from the conformational rearrangements that take place as the molecules aggregate. In the plot of chemical shift of water versus the concentration of partially hydrated SM, three linear relationships are seen, as shown in Fig. 7. In (a) at very low concentrations, both the upfield chemical shift ($\delta = 1.6$ ppm) of the water protons and the minimal change in δ with SM concentration suggest that these water molecules are not trapped within a reverse micelle. In region (b), the rate of change in chemical shift with SM concentration is more pronounced, and is interpreted as the progressive deshielding of the water protons as water molecules become trapped in the polar central pocket of the reverse micelles [35,36]. The intercept of these two lines can be used to estimate the critical micelle concentration (CMC). In the case of SM in $CDCl_3$, the CMC was evaluated to be (3.2 ± 0.3) mM at 32°C and 4.6 ± 0.4 mM at 42°C. Beyond this concentration, lipid–lipid interactions continued to become stronger as lipid–solvent forces were weakened. All resonances corresponding to the interface regions exhibited significant changes as the sample changed from a monomeric arrangement (below 3.2 mM) to reverse micelles (above 3.2 mM): the chemical shifts of the N**H** and O**H** resonance shifted downfield (solid symbols in Figs. 5 and 6, respectively) and the separation between the **H**1A and **H**1B resonances was reduced by more than a half (Fig. 4, solid symbols). All of these changes point to the formation of reverse micelles in which the interfaces of neighboring molecules are connected through H-bonds, either directly or through water bridges. The nature of these bonds is discussed later in this section.

Finally, for concentrations above ca. 50 mM, the rates at which the chemical shifts of the water (c in Fig. 7) and N**H** (Fig. 5) resonances changed with concentration were reduced by nearly an order of magnitude and suggest that above this concentration,

lipid–lipid interactions are near their maximal strength. This behavior differs from that inferred for DHSM in the accompanying paper. DHSM without the *trans* double bond between C4 and C5, exhibited a CMC of 13 mM at 50°C. Beyond this point, the aggregation process continued to impact the resonances of the interface region and bound water. The rate at which the chemical shift of the water resonance changed with DHSM concentration as aggregation took place (b in Fig. 7) was (5.02 ± 0.07) ppm per unit change in the logarithm of the concentration of DHSM (in mM) [33], more than twice larger than that for SM. The differences in the trends seen for DHSM and SM can be explained by the relative bulk of the two molecules: as the double bond of the SM molecule creates a kink in the conformation of the hydrophobic segment of the sphingosine chain, the volume occupied by SM is expected to be greater than that of DHSM. As a consequence, the interaction between neighboring molecules is expected to occur at lower concentrations for the bulkier SM as compared to DHSM. The same argument can be invoked to explain differences in the dependence of the rate of change of chemical shift of water with concentrations: SM molecules cannot come as close to each other as DHSM molecules can. As a consequence, the degree to which water protons are deshielded by the formation of H-bonds between lipids is not as high in SM as it is in DHSM. In other words, the reduced bulkiness of DHSM allows for stronger intermolecular interactions between neighboring molecules as compared to SM.

4.2. Fluid to gel state transition

The reverse micelles formed at concentrations above 3.2 mM at 32°C underwent a fluid to gel phase transition as the temperature was lowered. Visually, the clear, fluid samples became gels as the temperature was lowered. This transition results from the entanglement of the hydrophobic tails of neighboring micelles at the lower temperatures and has been observed for phosphatidylcholine dissolved in isooctane and cyclohexane [37,38], but not in chloroform [35,36]. As a result of enhanced van der Waals interactions, the sample becomes gelatinous and the spin–spin relaxation time T_2 is reduced, thus leading to the broadening of the spectral bands. Fig. 8 shows the changes in the linewidth of the C**H**$_2$ resonances as a function of temperature. As the highest concentration shown (125 mM), the temperature at which the gel phase was reached (T_g) was estimated to be 27 ± 1°C from the interpolation of the two straight lines drawn in the graph. At the lowest concentrations shown (3 mM) no significant broadening was observed. This indicates that below the CMC, the gelation of the sample cannot occur due to the extensive solvation of SM molecules. It is important to note that the value of T_g for DHSM at high concentrations was 37°C, 10°C higher than for SM. This difference in T_g points again to the relatively weaker strength of lipid–lipid interactions in SM assemblies as compared to DHSM.

4.3. Concentration- and temperature-dependent studies

As the monomers begin their aggregation, conformational changes take place and the nature of intra- and intermolecular hydrogen bonding interactions is altered. The discussion below addresses these changes and compares them to those seen for DHSM which are discussed in detail in the accompanying report [33]. It is important to emphasize that due to the long time scale of the NMR information, the discussion below pertains to average conformational preferences.

The difference in chemical shifts for the **H**″1A and B resonances of the partially hydrated choline head group suggests that, at concentrations below 5 mM (Fig. 2), the mobility of the head group is restricted to some extent, possibly because of intramolecular interactions in which the phosphate group participates. The separation of these resonances was also seen in DHSM at concentrations below 15 mM for the partially hydrated samples. In a fashion similar to that already reported for DHSM [33], the resonances did not overlap when the samples were dehydrated. It is therefore likely that the restriction which keeps **H**″1A and B in dissimilar magnetic environments in the absence of water may be lifted as water molecules bind to SM as the reverse micelles are formed. This restriction may be due to a weak intramolecular H-bond involving the methyl groups of the choline group and the anionic oxygens of the phos-

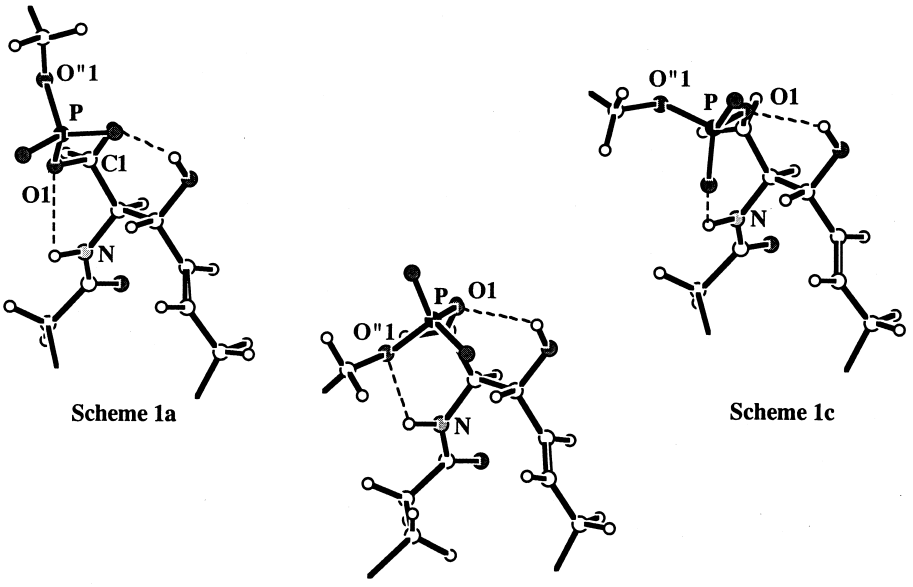

Scheme 1.

phate and/or an intramolecular H-bond between the NH group and the ester oxygen O″1. The former possibility has been supported in the literature by theoretical modeling studies of the phosphorylcholine head group in the gas phase [39]. In addition, modeling studies predict that increasing solvent polarity leads to the stabilization of an extended conformer in which the internal restriction is no longer present [40]. The coalescence of the **H**″1A and B resonances above the CMC supports this prediction.

Below the CMC it is also proposed that an intramolecular H-bond is formed between the NH moiety acting as a donor and an anionic and/or ester oxygens of the phosphate group as acceptors. This possibility is supported by the changes seen in the N**H** resonance in the partially hydrated and dehydrated samples (Fig. 5). Above the CMC, the presence of water resulted in an downfield shift of up to (0.15 ± 0.02) ppm in the N**H** resonance at the higher concentrations. We suggest that this deshielding of the NH proton is due to the partial breakage of the intramolecular H-bonds present below the CMC and the formation of intermolecular bonds between the NH groups and water molecules. These water molecules, in turn, can act as bridges between neighboring lipid molecules and participate in the H-bonding belt that leads to the formation of micelles.

This postulate is supported by the changes in the resonances corresponding to methylene protons **H**1A and B. The significant difference exhibited in their chemical shifts below the CMC, where the **H**1A and B resonances moved in different directions (downfield for **H**1A and upfield for **H**1B) to reach a difference of (0.36 ± 0.02) ppm, was reduced to (0.17 ± 0.03) ppm above the CMC for the partially hydrated samples. As water was removed, this difference was enhanced. Although these trends are comparable to those seen in DHSM below and above the CMC of 13 mM, the magnitude of the changes was greater for DHSM than for SM. In DHSM, the difference in chemical shifts between **H**1A and B decreased steadily up to about 80 mM, where a difference of 0.1 ppm was observed and retained at the higher concentrations. Correspondingly, the chemical shift of the N**H** resonance moved downfield rapidly with increasing concentrations up to a concentration of partially hydrated DHSM of 80 mM. In addition, the level of deshielding of the N**H** and bound water protons with increasing concentration was much greater in DHSM than in SM for the partially hydrated samples.

All of these trends suggest that, just as in DHSM, in the average monomeric conformation of SM, the NH moiety is involved in intramolecular H-bonding

interactions with either an ester oxygen (O1 in Scheme 1a or O″1 in Scheme 1b) or an anionic oxygen (Scheme 1c). These bonds would restrict the rotation of geminal protons **H**1A and B of the interfacial region (Scheme 1a–c) or the diastereotopic protons **H**″1A and B (Scheme 1b). As the concentration increases, some of these intramolecular bonds appear to be partially disrupted and the NH group becomes involved in intermolecular interactions with water molecules which act as H-bond acceptors and serve as bridges between lipid molecules. These water molecules are more tightly bound as the concentration of SM increases beyond the CMC (see Fig. 7).

The differences observed in the spectral trends exhibited by SM and DHSM suggest that it is not the nature but rather the degree or strength of the H-bonding interactions that differs in the two molecules and leads to weaker intermolecular interactions in SM assemblies. The chemical shifts for the N**H** moiety and bound water molecules in SM were consistently upfield from those in DHSM. Furthermore, the removal of bound water caused smaller upfield shifts in the N**H** resonance in SM (Fig. 5) than in DHSM (Fig. 6 in Ref. [33]). These differences suggest that the SM molecules cannot come as close together as DHSM molecules can. Therefore, the NH moiety remains, on average, more intramolecularly bound in SM as compared to DHSM. This postulate could account for the N**H** chemical shift never being as downfield in SM as it is in DHSM.

The lower strength of lipid–lipid interactions in SM can be partially attributed to the presence of the *trans* double bond between C4 and C5. This kink in the sphingosine chain may reduce the ability of neighboring molecules to come into close proximity. In turn, this leads to the possibility that the OH group on C3 is more sterically hindered in SM than in DHSM. This hindrance would reduce the possibility of participation of the OH group in intermolecular interactions that could, for example, connect the amide group of a SM molecule to the OH group of its neighboring lipid molecule via a water bridge.

The possibility of an intramolecular H-bond between the OH group and the ester oxygen O1 of greater strength in SM as compared to DHSM is supported by the behavior of the O**H** resonance. First of all, this resonance was narrower and easier to detect in SM than in DHSM. This suggests that the rate of exchange of the O**H** proton is slower in SM, as expected if this proton is more tightly held in an intramolecular H-bond. Secondly, its chemical shift was more downfield in SM than in DHSM, indicative of a greater deshielding effect, consistent with a stronger H-bond. Thirdly, the chemical shifts of the O**H** resonance were fairly similar for all concentrations above 5 mM and up to about 50 mM (Fig. 6). Beyond 50 mM, a gradual decrease in chemical shift was observed which could be attributed to the weakening of the intramolecular H-bonds as the lipid molecules come into close proximity. The rate of change in the chemical shift of the OH resonance with temperature did not vary significantly with concentration or hydration level. These observations suggest that the OH group is involved in an intramolecular bond in SM and only at concentrations above 50 mM, some of these internal bonds may be disrupted to form intermolecular H-bonds with either bridging water molecules or neighboring lipids. For the partially hydrated samples with concentrations below CMC, the upfield shift in the O**H** resonance (Fig. 6) could be due to the weaker strength with which water molecules surround this region of the molecule. Since the O**H** resonance was seen even in the dehydrated samples, it is postulated that water molecules are not necessary to establish the interaction between the OH group and the ester oxygen O1.

The behavior of the O**H** resonance in dehydrated samples of SM contrasts that seen for DHSM, for which this resonance could only be detected at high concentrations. It is proposed that this difference is due to greater strength with which the OH group is intramolecularly bound in SM. This stronger bond could explain the differences in chemical shift seen for the ^{31}P resonance for the two lipids. For all concentrations above 5 mM of both partially hydrated and dehydrated samples, the ^{31}P chemical shift was lower for SM than for DHSM. In fact, this difference in chemical shift is the very reason for which Glonek et al. [11] first recognized the presence of an unknown phospholipid in human lens membranes. This unknown lipid was identified by our group to be DHSM [13,14]. It is therefore proposed that the reason for this difference is the presence in SM of a stronger intramolecular bond which involves the OH group as donor and the ester oxygen O1 as acceptor, as shown in the schemes above. At concentrations

above 50 mM in the partially hydrated samples of SM, some of these intramolecular bonds may weaken as suggested by the upfield shift of the O**H** resonance (Fig. 6), the smaller difference in chemical shift between the **H**1A and **H**1B resonances and the increase in the ^{31}**P** NMR chemical shift (Fig. 3). In the dehydrated samples, and above 10 mM, neither the O**H** nor the ^{31}P resonance changed significantly with concentration. This suggests that the intramolecular bond is not weakened if water is not present and the bridging of neighboring lipid molecules through water molecules is precluded.

Below the CMC, the behavior of the chemical shift for the ^{31}P resonance changed dramatically for the partially hydrated samples. A maximum chemical shift of (0.86 ± 0.09) ppm was reached for the lowest concentrations of the partially hydrated samples (Fig. 3). This chemical shift of the ^{31}P resonance was higher than those observed for DHSM at all concentrations and temperatures. It is proposed that in the monomeric arrangement, water molecules cannot act as tight bridges between lipid molecules, as in the aggregated state. As a result, the NH group may be able to engage in a tighter intramolecular interactions with one of the anionic oxygens of the head group and the OH proton would be less deshielded in the less polar environment. Because of these intramolecular restrictions, a *trans-gauche* or *gauche-trans* arrangement of the phosphodiester torsional angles C1-O1-P-O″1 and O-P-O-C″1 could lead to the high value [41] of the chemical shift for the ^{31}P resonance. In the dehydrated samples at the lowest concentrations (below 10 mM), the downfield shift seen in the ^{31}P resonance for the partially hydrated sample did not occur (Fig. 3) and the OH group was more shielded than at the higher concentrations (Fig. 6). It appears that water molecules play an important role as active participants or mediators of the intramolecular H-bonds proposed for the partially hydrated samples in the monomeric form. The participation of water molecules in a cooperative H-bonding network is being pursued in our laboratory with molecular modeling and two-dimensional NMR methodologies. These studies are necessary for a quantitative description of the interactive roles that are played by the H-bonding sites in the interface of the SM molecule, the phosphate group and water.

4.4. Effect of hydration

The addition of water caused an upfield shift in the resonances corresponding to protons **H**″1, **H**″2, and $N^+(C\mathbf{H}_3)_3$ of the choline head group region (see Fig. 9). The changes in the interface proton resonances indicate that the restrictions that led to the separation in the **H**1A and **H**1B resonances were minimized as water was added and/or that the high polarity of water leads to greater magnetic equivalency for the environments of these two nuclei. It is possible that the intramolecular H-bond involving the NH moiety may be partially disrupted as excess water molecules are introduced. The immediate exchange of the NH group upon addition of D_2O indicates that the bond in which this group is involved is not very strong. In addition, the weaker intermolecular H-bonds in hydrated SM assemblies could account for the transition temperature of SM being 9°C lower than that for DHSM extracted from human lens membranes [42].

4.5. Conclusions

The presence of the double bond in SM appears to influence the strength of both intra- and intermolecular H-bonds. The results indicate the formation of an intramolecular H-bond between the OH group on C3 of the interface and the ester oxygen O1 of the phosphate group in SM. The strength of this bond is greater for SM than for DHSM. In addition, the conformational restriction imposed by this double bond does not allow neighboring lipid molecules to come as close as appears possible in DHSM. As a result, intermolecular lipid–water–lipid interactions in which the NH moiety interacts through water bridges with the interfacial region of a neighboring SM molecule, are not as strong as they are in DHSM assemblies. Molecular modeling and multidimensional NMR experiments which can establish internuclear distances are underway in our laboratory to confirm or negate the postulates presented in this report.

Acknowledgements

We gratefully acknowledge the National Eye Insti-

tute, which has supported this research through grant EY11657. We are indebted to Dr. Richard A. Porter for his helpful advice in the execution of NMR experiments.

References

[1] R.B. Gennis, in: Biomembranes: Molecular Structure and Function, Springer, New York, 1989, ch. 1.
[2] D. Voet, J.G. Voet, in: Biochemistry, Wiley, New York, 1995, ch. 11.
[3] J.L.W. Thudicum, in: A Treatise on the Chemical Constitution of the Brain, Bailliere, Tindall and Cox, London, 1884, p. 149.
[4] L. Pick, M. Bielchowsky, Klin. Wochenschr. 6 (1927) 1631–1637.
[5] D. Shapiro, H.M. Flowers, J. Am. Chem. Soc. 84 (1962) 1047–1050.
[6] P.F. Devaux, M. Seigneuret, Biochim. Biophys. Acta 555 (1979) 436–441.
[7] R.M. Broekhuyse, Biochim. Biophys. Acta 187 (1969) 354–365.
[8] G.L. Feldman, L.S. Feldman, G. Rouser, Lipids 1 (1966) 161.
[9] J.V. Grenier, D.B. Auderbach, C.D. Leahy, T. Glonek, Invest. Ophthalmol. Vis. Sci. 35 (1994) 3739–3746.
[10] S.R. Ferguson-Yankey, C.M. Talbott, L. Li, D. Borchman, M.C. Yappert, Invest. Ophthalmol. Vis. Sci. 38 (Suppl.) (1998) Abs. 3647.
[11] T.E. Merchant, J.H. Lass, P. Meneses, J.V. Greiner, T. Glonek, Invest. Ophthalmol. Vis. Sci. 32 (1991) 549–555.
[12] D. Borchman, W.C. Byrdwell, M.C. Yappert, Invest. Ophthalmol. Vis. Sci. 35 (1994) 3938–3942.
[13] W.C. Byrdwell, D. Borchman, R.A. Porter, K.G. Taylor, M.C. Yappert, Invest. Ophthalmol. Vis. Sci. 35 (1994) 4333–4344.
[14] S.R. Ferguson, D. Borchman, M.C. Yappert, Invest. Ophthalmol. Vis. Sci. 37 (1996) 1703–1705.
[15] I. Pascher, Biochim. Biophys. Acta 455 (1976) 433–451.
[16] I. Pascher, S. Sundell, Chem. Phys. Lipids 20 (1977) 175–191.
[17] I. Pascher, M. Lundmark, P.-G. Nyholm, S. Sundell, Biochim. Biophys. Acta 455 (1992) 339–373.
[18] K.S. Bruzik, Biochim. Biophys. Acta 939 (1988) 315–326.
[19] R.S. Khare, C.R. Worthington, Biochim. Biophys. Acta 514 (1978) 239–254.
[20] S.W. Hui, T.P. Stewart, P.L. Yeagle, Biochim. Biophys. Acta 601 (1980) 271–281.
[21] Y. Barenholz, T.E. Thompson, Biochim. Biophys. Acta 604 (1980) 129–158.
[22] Y. Barenholz, J. Suurkuusk, D. Mountcastle, T.E. Thompson, R.L. Biltonen, Biochemistry 15 (1976) 2441–2447.
[23] W.I. Calhoun, G.G. Shipley, Biochim. Biophys. Acta 555 (1979) 436–441.
[24] P.R. Maulik, P.K. Spirada, G.G. Shipley, Biochim. Biophys. Acta 1062 (1991) 211–219.
[25] G.G. Shipley, L.S. Avecilla, D.M. Small, J. Lipid Res. 15 (1976) 124–131.
[26] K.S. Bruzik, M.-D. Tsai, Biochemistry 26 (1987) 5364–5368.
[27] J.M. Boggs, Biochim. Biophys. Acta 906 (1987) 353–412.
[28] L.K. Li, L. So, A. Spector, J. Lipid Res. 26 (1985) 600–609.
[29] L.K. Li, L. So, A. Spector, Biochim. Biophys. Acta 987 (1987) 112–120.
[30] K. Simons, E. Ikonen, Nature 387 (1997) 569–572.
[31] R.E. Brown, J. Cell Sci. 111 (1998) 1–9.
[32] N.M. Hooper, Mol. Membr. Biol. 16 (1999) 145–156.
[33] S.R. Ferguson-Yankey, D. Borchman, K.G. Taylor, D.B. DuPré, M.C. Yappert, Biochim. Biophys. Acta 1467 (2000) 307–325.
[34] M.L. Sparling, R. Zidovetzki, L. Muller, S.I. Chan, Anal. Biochem. 178 (1989) 67–76.
[35] G. Datta, P.S. Parvathanathan, U.R.K. Rao, K. Deniz, U. Physiol. Chem. Phys. NMR 24 (1992) 51–61.
[36] R. Hague, I.J. Tinsley, S. Schmedding, J. Biol. Chem. 247 (1972) 157–161.
[37] D. Capitani, E. Rossi, A.L. Segre, Langmuir 9 (1993) 685–689.
[38] D. Capitani, A.L. Segre, F. Dreher, P. Walde, P.L. Luisi, J. Phys. Chem. 100 (1996) 15211–15217.
[39] J. Landin, I. Pascher, D. Cremer, J. Phys. Chem. 99 (1995) 4471–4485.
[40] J. Landin, I. Pascher, D. Cremer, J. Phys. Chem. 101 (1997) 2996–3004.
[41] D.G. Goldstein, in: Phosphorus-31 NMR, Principles and Applications, Academic Press, Orlando, FL, 1984, pp. 9–23.
[42] D. Borchman, W.C. Byrdwell, M.C. Yappert, Ophthalm. Res. 28 (Suppl. 1) (1996) 81–85.